

FAST FACTORISED BACKPROJECTION ALGORITHM FOR PROCESSING OF SAR DATA

Per-Olov Fröling Department of Radar Systems, Swedish Defence Research Agency (FOI)
Lars M. H. Ulander Department of Radar Systems, Swedish Defence Research Agency (FOI)
Daniel Murdin Department of Radar Systems, Swedish Defence Research Agency (FOI)

1 INTRODUCTION

Synthetic aperture radar (SAR) (or sonar (SAS)) is a method for generating high-resolution radar (sonar) maps. This technique has been extensively used for high resolution imaging in the last decades. In the early days, data processing was carried out by holographic techniques using a complex arrangement of lasers and lenses. Today's processing exploit fast computers that makes it feasible to incorporate additional algorithm complexity, which is needed to include more general imaging situations.

One of the driving forces of the development of SAR image formation has been to obtain higher image resolution. Wider transmitted bandwidth achieves higher range resolution. Either a higher centre frequency or wider aspect angle variation will improve azimuth resolution, which stresses the motion compensation abilities of the SAR algorithm, as well as an increased computational load due to the larger data set to process.

Recently developed fast factorized time domain backprojection algorithms^{1,2,3} have shown great success for airborne wide-angle and ultra-wideband low-frequency SAR data. Computational complexity is close to that of Fourier-based algorithms, i.e. Fourier-Hankel or Range Migration (ω -K). For linear flight tracks, backprojection and Fourier methods give similar results but for curved tracks backprojection has a significant advantage since the correction are implicit in the algorithm.

We have recently showed that the image quality generated by the fast factorized backprojection algorithm depends on the accuracy of the interpolation kernels², using simulation which assumes ideal straight flight tracks. Image quality can be made arbitrarily close to the ideal performance provided that interpolation in both range and angle is performed with controlled accuracy.

The earlier developments have been targeted at airborne wide-angle and ultra-wideband SAR systems. In this paper, we address new issues which come up when the fast factorized backprojection algorithm is applied to SAR systems with narrower azimuth beamwidths and the complexity of curved tracks. Both stripmap and spotlight geometries are considered.

The deviation from a straight line is as said above inherent in the processing algorithm and will only introduce distortions on sidelobe structure of the impulse response. For managing narrower beamwidths the main modification which needs to be introduced is limiting the backprojection to be within the physical antenna beamwidth. In principle, this would be unnecessary provided that the SAR image pixels size is reduced to support the high angular bandwidth. Data belonging to angles outside the antenna beam could then be filtered as a post-processing step followed by downsampling. However, in many cases this would result in excessively small pixel sizes and a large computational overhead. We therefore propose a modified algorithm with beam-limited backprojection for the stripmap case. For the spotlight case, the beam-limitation is also preferred but needs to also include a rotating azimuth beam.

2 FAST FACTORIZED BACKPROJECTION (FBP) THEORY AND IMPLEMENTATION TECHNIQUES

2.1 FBP polar implementation

A fast time-domain algorithm which provides a controllable compromise between speed and image quality has been developed². In this paper we show results from a fast factorized backprojection algorithm (FBP) based on using a polar coordinate system in the intermediate factorizing stages and a cubic interpolation kernel in angular domain.

The fast time-domain processing algorithms are based on the original one-stage global backprojection¹, where all image pixels are individually integrated using the received radar data from all flight track positions.

The FBP algorithm is initialized by processing very small sub-apertures in a first step, and thus the resulting integrated data have very poor azimuth resolution. In a next step we can reuse the integrated beams for forming new beams with higher angle resolution by merging sub-apertures into larger sub-apertures. This procedure is continued until the final image resolution is reached.

The number of operations required for the image formation using an aperture with L positions, M^2 image pixels and n sub aperture positions used for generating new beams at each factorization stage, is known to be proportional to $n \times M \times L \times K$. Typically n is chosen to be equal to the K -th square root of L . Consider n equal to two, i.e. $2 \times M \times L \times \log_2 L$, which directly competes with the well-recognized fast Fourier methods.

In practice, however, it is convenient to block the processing of the entire synthetic aperture length into smaller segments in order to relax the memory requirement or as it shows for more optimal narrow beam processing. The blocking procedure also makes it feasible for continuous image output of segments in a stripmap mode processing, corresponding to the block size.

2.2 Processing stages

The image formation starts off with generation of low resolution beams based on a few data records from neighboring aperture positions, see Figure 1.

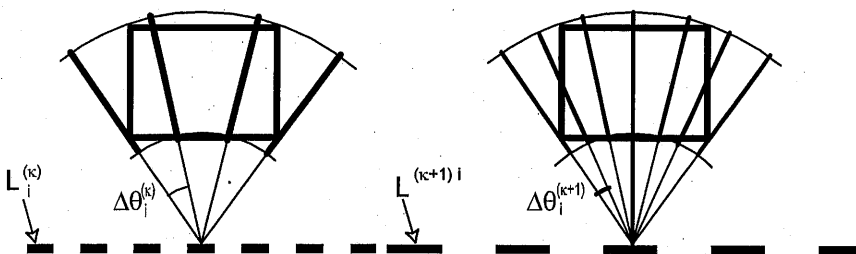


Figure 1. Illustration of two factorization steps with doubled sub-aperture lengths and increased number of azimuth beams covering the image area.

The beam angle separations are based on the bandwidth of the backprojected data. In order to refine the azimuth interpolation, an oversampling is selected to trade image quality against computational load.

An azimuth interpolation kernel is introduced into each beam-forming step for reducing the interpolation error of the new beams placed inbetween as illustrated in Figure 2.

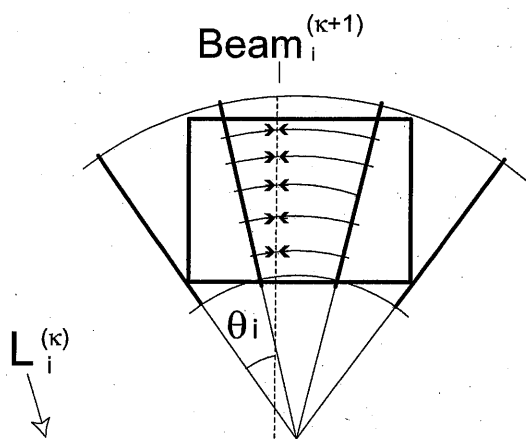


Figure 2. The dashed line illustrates the linear interpolation of a new sub-aperture beam derived from the previous factorizing step.

The azimuth sampling rate is based on the angular bandwidth, B_θ , which is determined from the maximum angular frequency according to²

$$B_{\theta, \max} = \begin{cases} 4k\Delta x : \Delta x < R \\ 4kR : \Delta x > R \end{cases}$$

where k is the maximum transmitted wavenumber, Δx is the sub-aperture length from the new phase centre, R is the polar grid near range, see Figure 3.

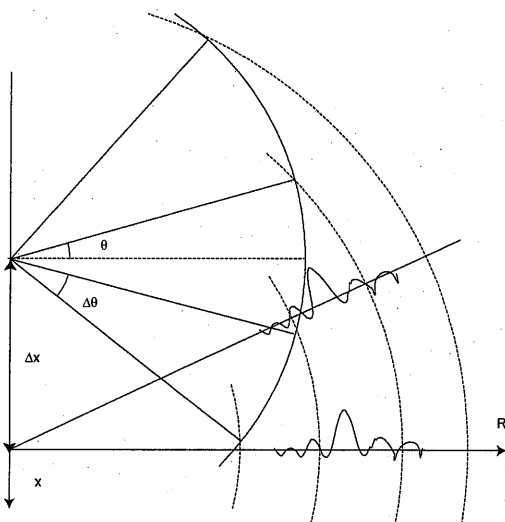


Figure. 3 Range data transformation from a sub-aperture position to a new phase centre using an angular sampling rate of $\Delta\theta$.

In order to comply with memory restrictions the total aperture can be divided into blocks where the image formation will be processed through all the factorizing steps until next block is processed. Two factorizing steps data has to be kept in the memory, the new and the former one. The available memory size on the processing computer defines the maximum block size.

Earlier results from image processing based on simulation of omni-directional antenna pattern have showed that an oversampling of $4 B_0$ combined with a cubic interpolator produces results close to an ideal impulse response in the azimuth direction. The examples given in this paper for narrow beam systems are therefore also based on using these parameter settings.

One additional change from the original implementation is to introduce beam boundaries in the backprojection³. If not, the data will be backprojected over a larger image area than being illuminated. This will introduce "ghost" targets with an angle separation according to the PRF of the SAR data acquisition. When the image pixel sampling rate is adequate this data can be filtered out as a second processing step but will introduce additional computational overhead as well as the unnecessary processing from backprojection of data beyond the physical beam width. The limitation of the backprojected SAR data corresponding to the physical beam width is here introduced only in the first factorization steps. In the proceeding steps the data is processed as in the original implementation covering the entire processed angle sector. However, as the processing proceeds azimuth directivity is obtained and the data at higher Doppler angles than the physical beam width will be suppressed. However it is convenient to utilize the block processing technique in order to reduce the final aspect angle variation which is defined by the original beamwidth plus the processed aperture length, see Figure 4.

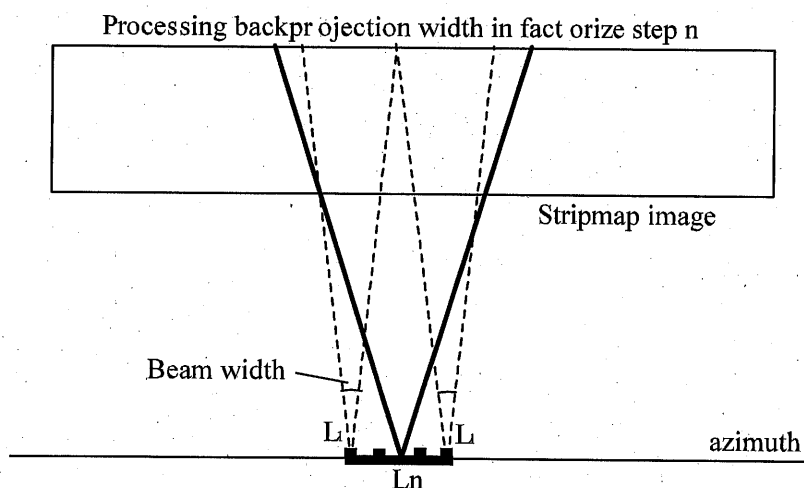


Figure 4. Illustration of the backprojection azimuth angle coverage for different factorizing steps. The first factorizing step sub-aperture L_1 is limited to match the physical beamwidth while a proceeding step subaperture, L_n , has to include all angles in the earlier steps.

2.3 Simulations

We simulate the SAR data corresponding to a microwave system operating at 10 GHz using a bandwidth of 240 MHz. We determine the ideal point target response for a pulse compressed FM-chirp pulse using $2.5 \mu\text{s}$ pulse. The incidence angle to image centre is 60° . The motion compensation is applied for a horizontal nominal focusing height which has a perfect match at the point target position. The beamwidth is set to be 1.6° with a Gaussian shape. In the spotlight mode the target is illuminated over an aspect angle variation of 8° . The processing has been made by the original tested implementation without beam limitation and the suggested limitation in the first factorizing step. The image formation has also been analyzed for linear and curved track. The curved track is defined by 1.5 period of a sine curve with amplitude of 2.5 m along the total aperture length, see Figure 5.

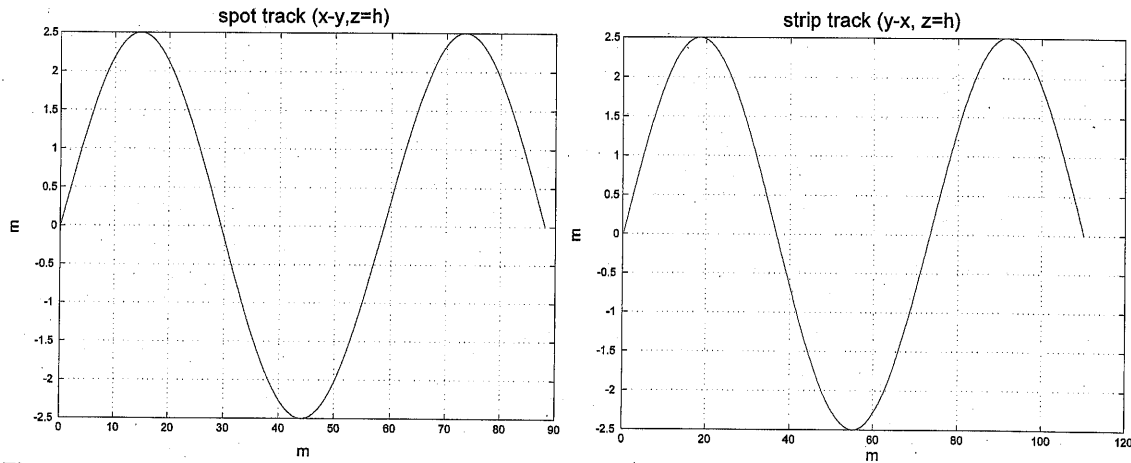
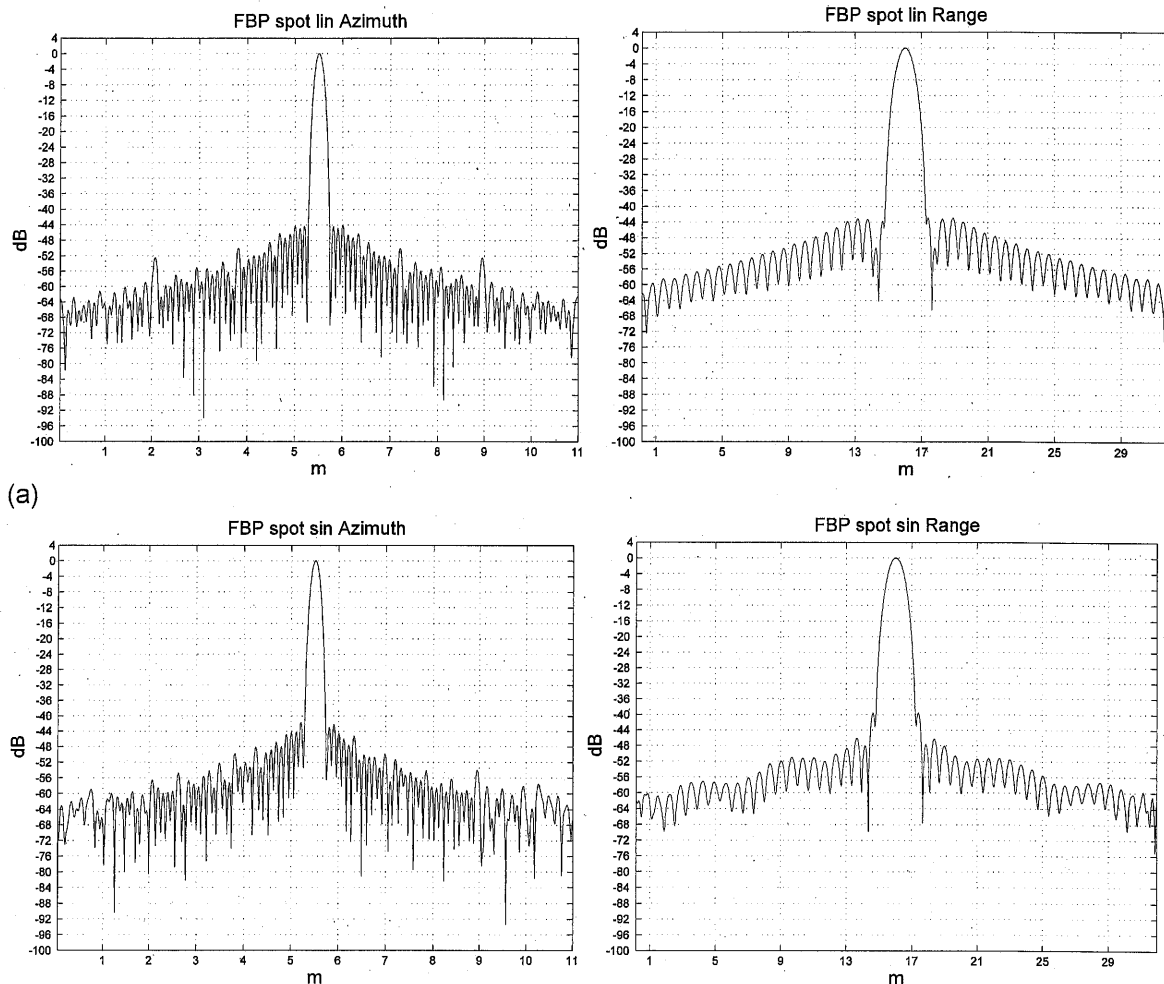


Figure 5. The shape of the curved track in the horizontal plane, x-y, for spot and stripmap mode respectively. The flight height is constant in both cases.

The geometries have been scaled to generate short processing times and the entire aperture length is 8 m and 110 m for spot- and stripmap mode, respectively. The effective aperture length in stripmap mode is 22 m. The processing has in both cases been blocked into 4 aperture blocks.

3 RESULTS

Plots in range and azimuth direction of the resulting impulse responses are illustrated in Figure 6-7. The spotlight mode using linear and curved track is illustrated in Figure 6. We can see that the sidelobe structure is somewhat influence by the processing technique using linear track and which is slightly further distorted by the curved track simulations.

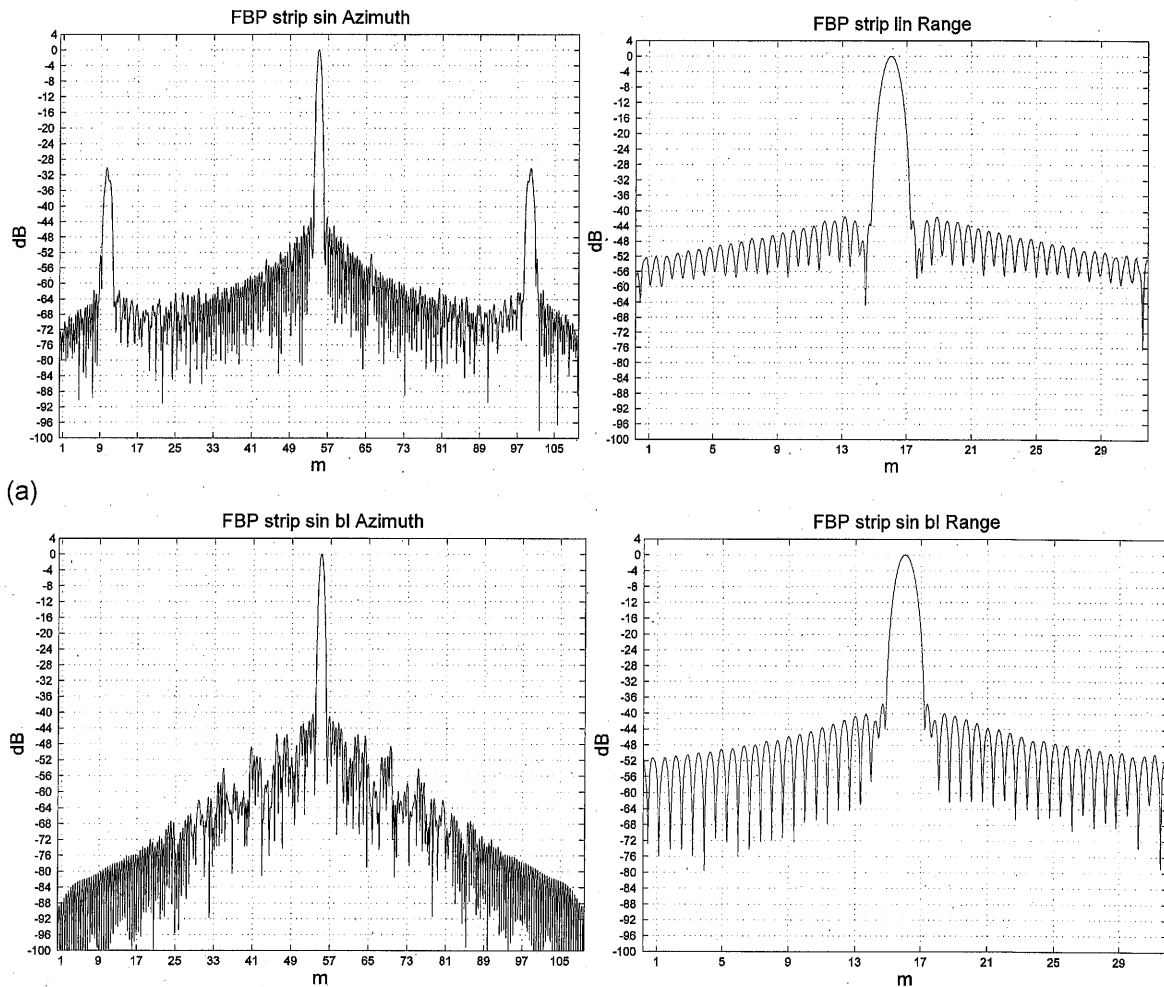


(b)
Figure 6. Impulse response from spotlight mode using linear track (a) and curved track (b).

In Figure 7(a) the use of the original unlimited backprojection over the entire image results in azimuth ambiguities with an angular separation corresponding to the selected PRF of the SAR data acquisition. This occurs despite the PRF matches the physical beamwidth.

The ambiguities disappears when the limitation of the backprojected data in the first factorizing step corresponding to the physical beamwidth is introduced, see Figure 7(b). Although the ambiguities are suppressed the sidelobe structure is distorted and somewhat increased both in range and azimuth in a way that is not yet fully understood.

The resolution in range and azimuth follows closely the expected values, see Table 1. Theoretical resolution, when using a Hamming window in range-frequency and Doppler cone angle, is in range 0.81 m and in azimuth, 0.14 m and 0.67 m for spotlight and stripmap mode, respectively. The side lobes levels are expected to be around -43 dB.



(a) The impulse response using the original unlimited angular backprojection. Azimuth ambiguities will occur corresponding to the data acquisition PRF. (b) The introduced limitation of the backprojected data to correspond to the physical beam width in the first factorizing step.

Table 1.

Mode ¹ Original FBP ² Beam limited FBP	3dB width range (m)	3dB width azimuth (m)	Peak sidelobe range (dB)	Peak sidelobe azimuth (dB)
Spot linear track	0.82	0.14	-44	-43
Spot curved track	0.82	0.14	-42	-40
Strip curved track ¹	0.83	0.67	-43	-42
Strip curved track ²	0.83	0.69	-40	-38

4 CONCLUSIONS

We have described an implementation of a fast factorized time domain back projection algorithm for narrow beam SAR imaging. The results show that by using a four point cubic interpolation kernel and an appropriate angular sampling rate we obtain good impulse response, in the terms of sidelobe performance and resolution figures, with the benefit of the reduction of the required number of operations using a fast backprojection algorithm in the time domain. The effects of a

curved track and the required motion compensation in the factorizing steps seem not to distort the results substantially for reasonable track deviations. This shows that the fast factorized backprojection can be applicable to microwave SAR imaging with narrow antenna beamwidths.

5 REFERENCES

1. L.M.H. Ulander, H. Hellsten and G. Stenström, 'Synthetic Aperture Radar Processing using Fast Factorised Back-Projection', IEEE Trans., Aerospace and Electronic Systems, Vol. 39, no 3, 760-776. (2003).
2. P.-O. Fröling and L.M.H. Ulander, 'Evaluation of angular Interpolation Kernels in Fast back-Projection SAR processing', IEE Proceedings Radar, Sonar and navigation, Vol. 153, Issue 3, 243-249. (2006)
3. L.M.H. Ulander, P.-O. Fröling, and, D. Murdin, 'Fast Factorised Backprojection Algorithm for Processing of Microwave SAR Data', Proc. EUSAR 2006, 16-18 May 2006, Dresden, Germany, 4 pp., (2006)